Proton Effects on Diazafluorene Derivatives with Sulfur-Rich Substituents, a Structural, Spectroscopic and Theoretical Study

Lei Yu,[†] Qin-Yu Zhu,*[,†,‡] Yong Zhang,[†] Zhi-Xin Lei,[†] Gai-Yan Niu,[†] and Jie Dai*[,†,‡]

Department of Chemistry and Key Laboratory of Organic Synthesis of Jiangsu Province, Soochow University, Suzhou 215123, People's Republic of China, and State Key Laboratory of Coordination Chemistry, Nanjing University, Nanjing 210093, People's Republic of China

Received: August 15, 2008; Revised Manuscript Received: October 21, 2008

Proton effects on an intramolecular donor−acceptor molecular system 4′,5′-diaza-9′-(4,5-dialkylthio-1,3-dithiol-2-ylidene)fluorenes (methylthio = L^1 (**1**), ethylthio = L^2 (**2**)) have been experimentally and theoretically studied. Structures of L^2 (**2**) and three protonated salts, $[L^2 \cdot H]CF_3SO_3$ (**3**), $[L^1 \cdot H]CF_3SO_3$ (**4**), and $[L^1 \cdot H]ClO_4$ (**5**), were characterized by single-crystal X-ray determination. In all these salts the cations are found to be monoprotonated even in an excessive amount of acid. The protonated imine group forms strong N−H···O or N−H···N hydrogen bonds, which enhance the interaction between cations and anions and play an important role in the molecular packing. The measurement of UV−vis spectra indicates a two-step red shift of the absorption bands, which corresponds to the two-step protonation of L in solution. The intramolecular charge-transfer (ICT) property is enhanced when the compounds are protonated. Compound L is also a proton sensible fluorescent system with two-step remarkable changes in band energy and intensity. The study on the effect of protonation is further complemented by theoretical calculation with the DFT/TDDFT method.

Introduction

Bipyridine (bipy) and 1,10-phenanthroline (phen) as chelate ligands have attracted great attention due to their excellent electronic properties: good σ electron donor and π electron acceptor. Although numerous transition metal complexes with derivatives of bipy and phen have been reported, these ligands have been widely used until now.[1,2] The design and synthesis of new derivatives of bipy and phen or their analogues and the study of their electronic and photophysical properties are particularly interesting for their potential applications in material chemistry.[3−5] Diazafluorene derivatives have been considered as very promising molecules for their luminescence properties, intramolecular or intermolecular charge transfer, and ability to coordinate metal ions like phen and bpy. We have recently investigated a series of new derivatives of diazafluorene, the compounds 4′,5′-diaza-9′-(4,5-dialkylthio-1,3-dithiol-2-ylidene)-fluorenes (methylthio = L^1 (**1**), ethylthio = L^2 (**2**)) (Scheme 1).[6] The moiety of 4′,5′-diazafluorene has a similar structure to that of 1,10-phenanthroline and 2,2′-bipyridine, and it is further conjugated with a sulfur-rich moiety of 4,5-dialkylthio-1,3-dithiol-2-ylidene, which is an electron donor unit with a C_2S_4 core. Some coordination complexes with this type of ligand have been synthesized and characterized crystallographically. However, as a new kind of D−A compound, the electronic structure and the intramolecular charge-transfer (ICT) property[7] have not been revealed yet.

Huang et al. studied the protonation of bipyridine and its derivatives and found that positive charges on the proton play a very important role in the modification of the electronic structures of the molecules.[8] Armaroli et al. have also extensively investigated substituted phenanthrolines and their protonated forms.[9] They have found that the substitute pattern of the phenanthroline core and the acidity of the environment tuned the molecular photophysical properties. Protonation of the nitrogen atoms induces positive charge into the system, which may affect the electronic properties. On the other hand, hydrogen bonding becomes complicated in these systems by protonation, which results in the enhancement of intramolecular or intermolecular interactions and consequently influences the electronic properties of the molecules.

SCHEME 1: Scheme of the Compounds with Denominate Labeling

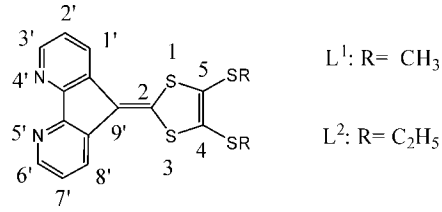

In our previous work, we have reported the proton effect on an intramolecular donor−acceptor molecular system, TTF-pyH^+.[10] As a sequential work, we now turn to consider the new protonated system of L^1 and L^2. Unlike the former, this kind of compound undergoes a two-step protonation. Its effect on intramolecular charge transfer (ICT) was investigated by electronic spectra and ^{1}H NMR spectra. Fluorescence response on the two-step protonation has also been discussed. Crystal structures of unprotonated and protonated compounds are presented herein to help in understanding the H···L integration. A theoretical study at the density functional theory (DFT) level has been done to complement the experimental results.

Results and Discussion

Description of the Crystal Structures: L^2 (2). The crystal structure of compound **2** is shown in Figure 1a. In **2** there are

* Corresponding authors. E-mail: daijie@suda.edu.cn and zhuqinyu@suda.edu.cn. Fax: +86 (0)512 65880089.
† Soochow University.
‡ Nanjing University.

10.1021/jp8073283 CCC: $40.75
Published on Web 12/02/2008

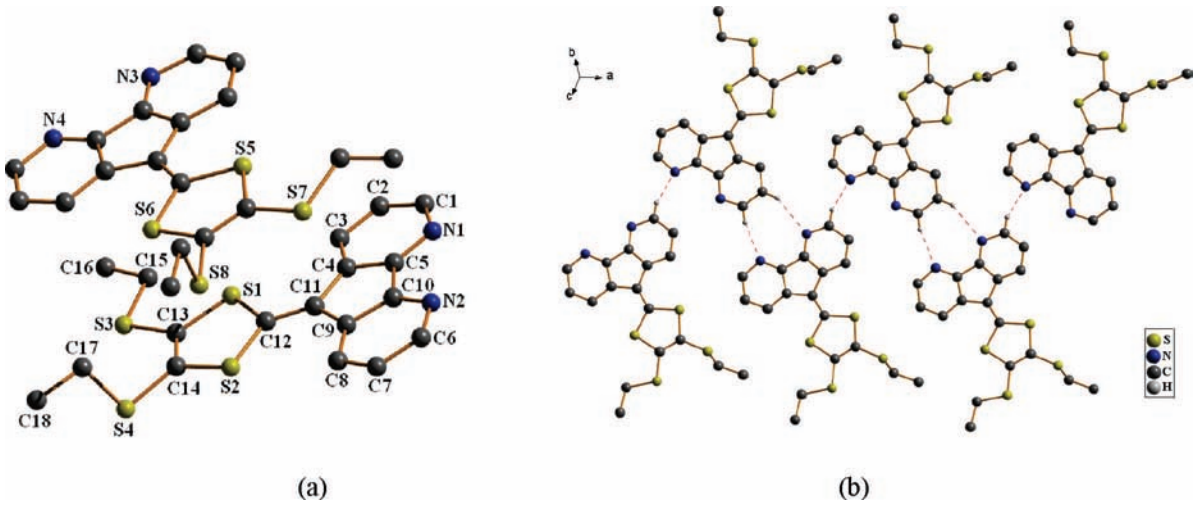

Figure 1. (a) Crystal structure of **2** with selected labeling scheme, hydrogen atoms being omitted for clarity. (b) 1-D band structure of **2** along the *a* axis, arranged with weak N···H−C bonds.

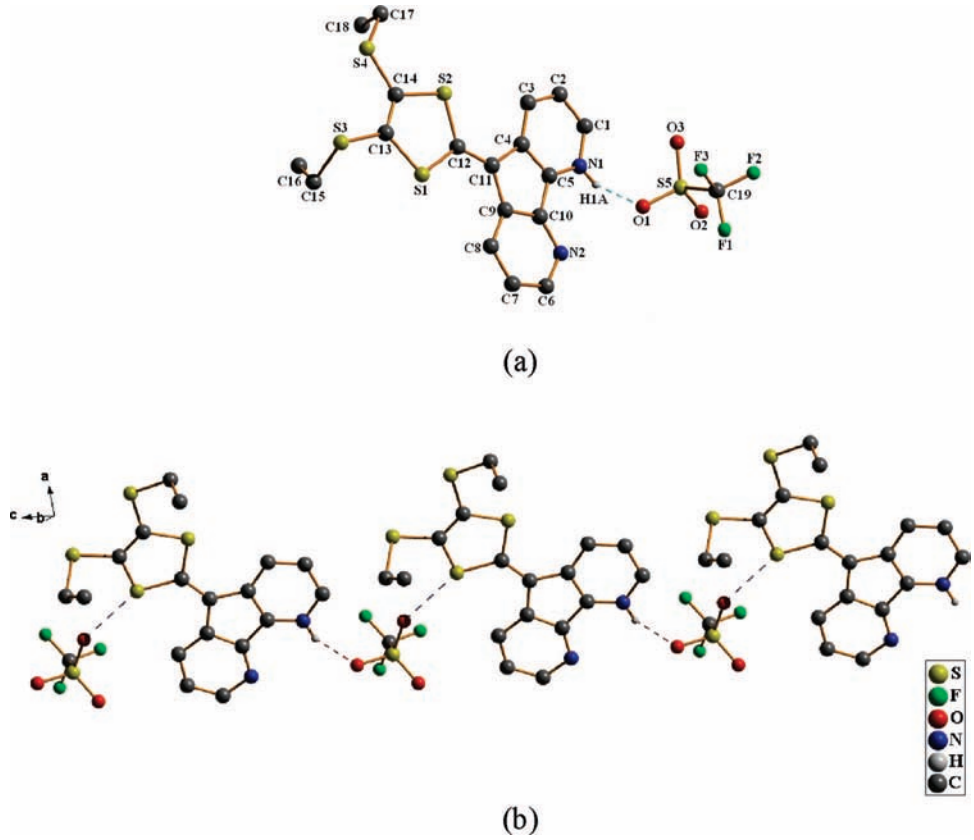

Figure 2. (a) Crystal structure of **3** and (b) the chain structure along the *c* axis, connected through O···H−N and O···S interactions. Only the hydrogen atom of N−H is presented and two of the disordered C17′, C18′ atoms have been omitted for clarity.

two kinds of molecules, A and B, with different symmetry. The atoms of the molecule, except two ethyl groups, are conjugated in a quasiplane. The mean deviation from the plane of the two molecules A and B is 0.0323 and 0.0270 Å, respectively. Molecules A and B are alternately arranged with weak N···H−C bonds forming a 1-D band structure along the *a* axis (Figure 1b). By weak S···S and C···S short contacts as well as N···H−C bonds, the chains further construct a 2-D layer structure (Figure 1 in the SI).

$[L^2 \cdot H]CF_3SO_3$ (3). The molecular structure of **3** is shown in Figure 2a. The proton was observed experimentally on one of the two nitrogen atoms of the diazafluorene with slight change in the bond distances of N−C in the heterocyclic ring. The atoms of the cation, except two ethyl groups, are conjugated in a quasiplane. The mean deviation from the least-squares plane is 0.0991 Å. The bond distance C5−C10 between the two pyridine rings in this compound is shorter (1.448(4) Å) than that found in the parent molecule **2** (1.458(5) Å). The C1−N1−C5 angle increases by 6.3° compared with those in **2** while the C6−N2−C10 angle is almost equivalent. There is strong O···H−N hydrogen bonding between the cation and the anion with an O···N distance of 2.729(3) Å. On the other hand, short contacts are observed for O3···S1 with a distance of 3.233(3) Å. Connected through these O···H−N hydrogen bonds and O···S contacts, a chain structure along the *c* axis is formed (Figure 2b). Two neighboring chains are further contacted each

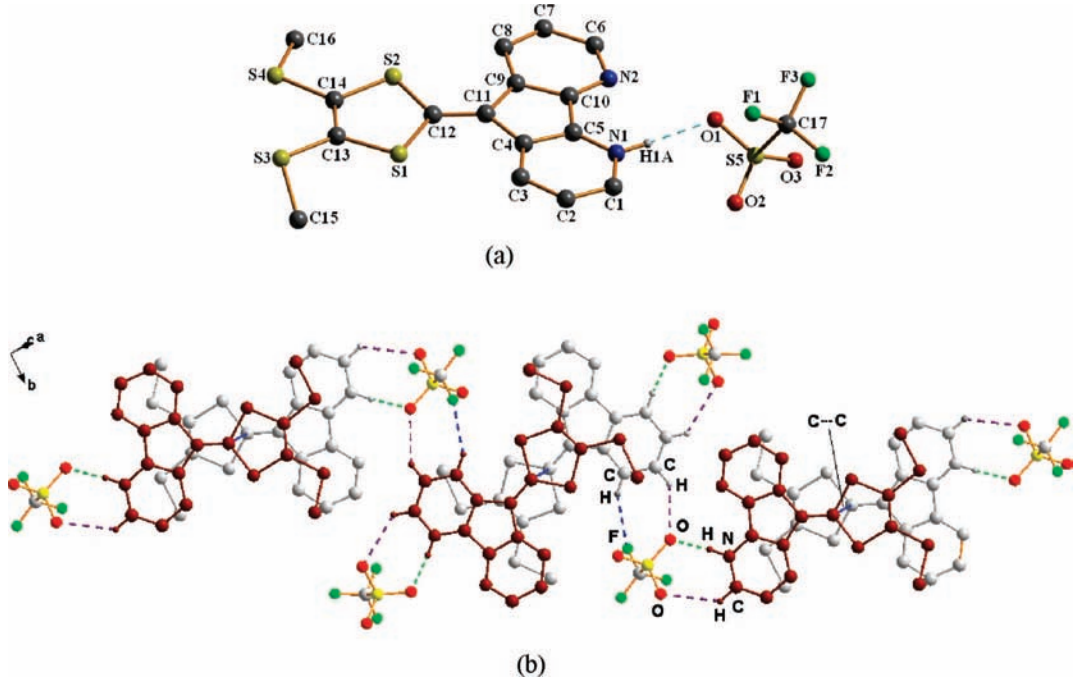

Figure 3. (a) Crystal structure of **4** with labeling scheme, only the hydrogen atom of N−H is presented for clarity. (b) Packing diagram of protonated cations and anions in **4,** showing the important H-bonds and C···C stacking.

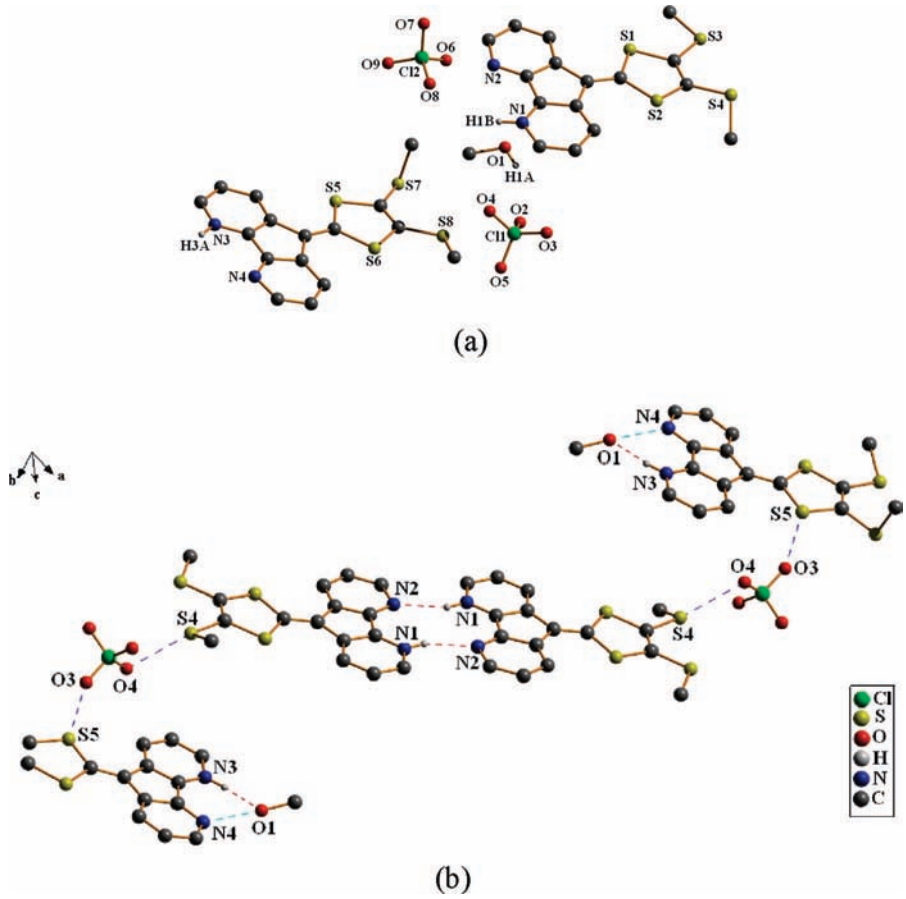

Figure 4. (a) Crystal structure of **5** with selected labeling scheme, only the hydrogen atom in N−H is presented for clarity. (b) Interactions in **5** showing the B−C−A−A−C−B arrangement.

other by C···C interactions to form a two-layer chain structure (Figure 2 in the SI).

$[L^1 \cdot H]CF_3SO_3$ (4). The structure of compound **4** closely resembles that of **3** (Figure 3a). As for compound **3**, in **4** one of the nitrogens of the cation is protonated and is hydrogen bonded to the oxygen of the anion (O···H−N). Except for two methyl groups, the atoms in cation are conjugated in a quasiplane with mean deviation 0.0728 Å. However, the crystal system and weak interactions of **4** are different from those of **3**. Short C···C intermolecular stacks

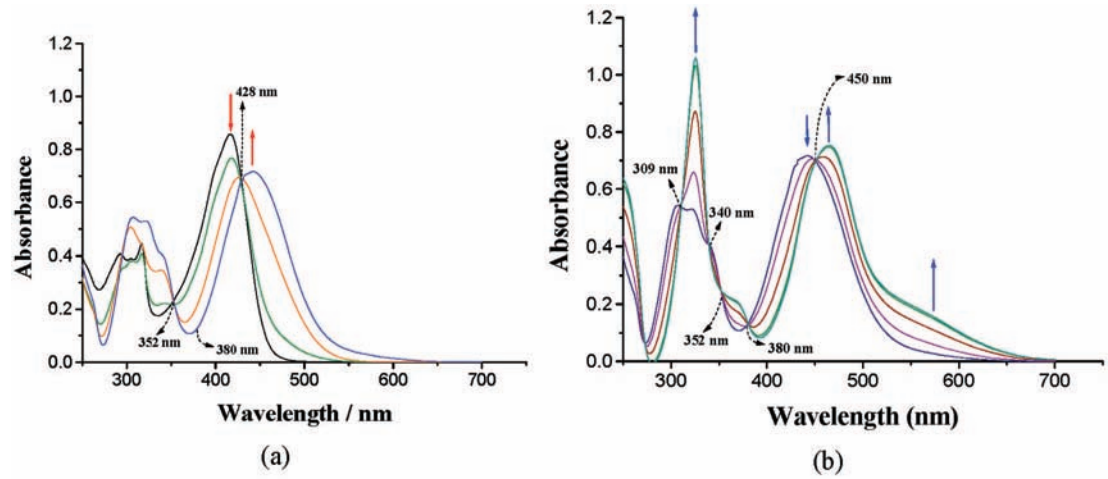

Figure 5. Changes of the absorption of a 2.0×10^{-4} M solution of L^1 in CH_2Cl_2 upon addition of increasing amounts of CF_3SO_3H: (a) from 0 to 2.0×10^{-4} M and (b) from 2.0×10^{-4} to 4.0×10^{-4} M. Dashed arrows indicate isosbestic points.

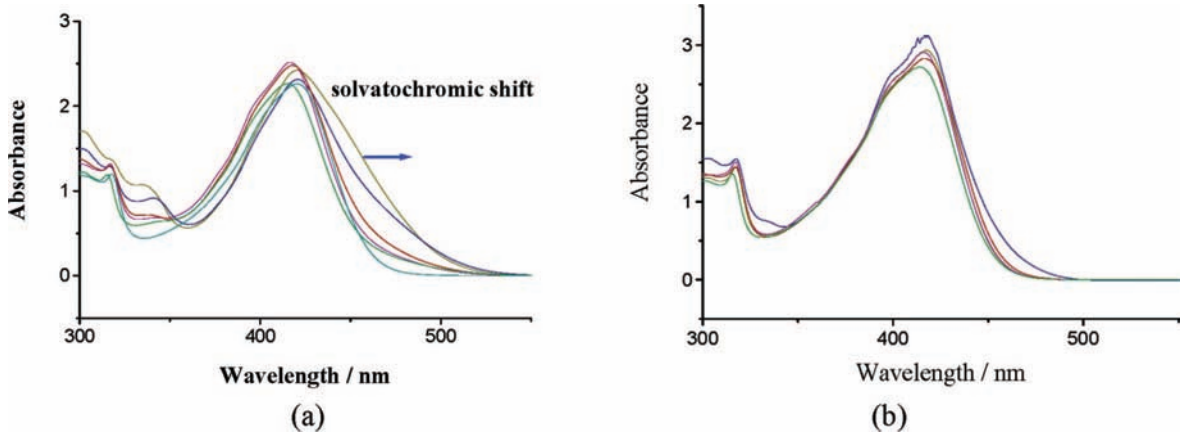

Figure 6. (a) Solvatochromic shifts observed in the spectra of compound **4** ($L^1 \cdot H^+$) in solvents with varying polarity (from left to right: MeCN, EtOH, MeOH, CH_2Cl_2, and CH_3Cl); (b) spectra of L^1 in solvents with varying polarity (from left to right: MeCN, EtOH, CH_3Cl, MeOH, and CH_2Cl_2).

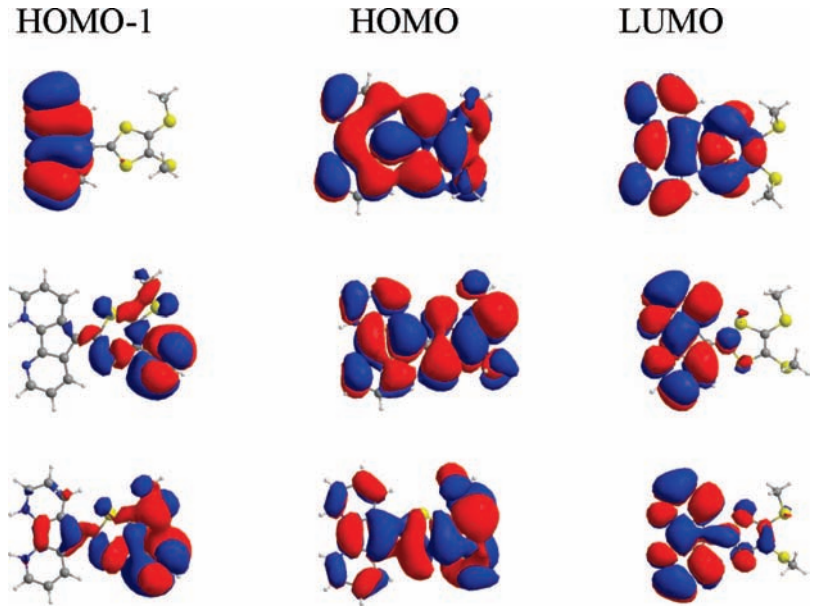

Figure 7. Frontier orbitals calculated for L^1 (top), $L^1 \cdot H^+$ (middle), and $L^1 \cdot H_2^{2+}$ (bottom).

(3.380 Å) assemble the cations to dimeric pairs (Figure 3b) and effective C−H···F and C−H···O weak hydrogen bonds are observed. Cooperating with the O···H−N hydrogen bond mentioned above, these interactions arrange the cations and anions to a 2-D extended double-layered supramolecular structure (Figure 3b).

$[L^1 \cdot H] \cdot ClO_4$ (5). The molecular structure of **5** is shown in Figure 4a. Although the proton has not been observed directly

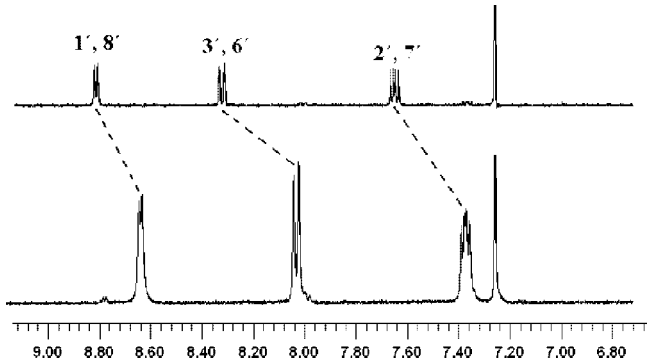

Figure 8. ^{1}H NMR of parent compound **2** (bottom) upon addition of acid (top) in $CDCl_3$.

from the Fourier map in compound **5**, it has been ridden to one of the imine N atoms, analogous to **3** and **4**. No hydrogen bond exists between cation and anion, which is different from the analogue [dafone$H^+(ClO_4)$][11] (dafone = 4,5-diazafluorene-9-one). In the crystal structure of **5**, there are two cations A and B as well as two anions C and D with different symmetry in the crystal. The mean deviations from plane of the two cations are 0.0546 and 0.0539 Å, respectively. Double hydrogen bonding interactions are the most important feature in the structure of **5**, which contributes significantly to the staggered arrangement of B−C−A−A−C−B (Figure 4b). The formation of double hydrogen bonding between molecules A, not the cation−anion H-bond found in **3** and **4**, suggests the weaker interaction of N−H···O (ClO_4^-) compared with that of N−H···O ($CF_3SO_3^-$). The cation of B is hydrogen bonded to the cocrystallized methanol oxygen.

Electronic Absorption Spectrum and the ICT Transition. As a conclusion of the X-ray crystal structure determination, the monoprotonated salts are the favorite products in the solid state, even being isolated from two equivalent acids. Figure 5 shows the electronic absorption spectra of compound L^1 in CH_2Cl_2 upon addition of increasing amounts of acid CF_3SO_3H. Besides the weak absorption bands at 292, 312 nm, the parent compound L^1 has a strong absorption at 417 nm (black line). At first addition of increasing amounts of CF_3SO_3H to L^1 in CH_2Cl_2 (from 0 to 1 equiv) leads to the disappearance of the band at 417 nm and to the development of a new band at 440 nm. Isosbestic points are clearly observed at 352 and 428 nm. The appearance of isosbestic points reveals that there is a two-species equilibrium in this system. They are the parent compound L^1 and the monoprotonated compound $L^1\cdot H^+$. Upon further addition of the acid (from 1 to 2 equiv), new band at 464 nm appears and the band at 440 nm disappears. Meanwhile neat isosbestic points at 309, 340, 380, and 450 nm are observed, which confirms a new equilibrium between monoprotonated species $L^1\cdot H^+$ and diprotonated species $L^1\cdot H_2^{2+}$. That is to say a diprotonated species exists in solution with higher acidity. No changes in the absorption spectra are observed upon further addition of acid, so the protonation is fully completed.

More finely, shoulder peaks can be observed at about 500−550 nm for $L^1\cdot H^+$ (an unsymmetrical tail of the 440 nm band) and about 580 nm for $L^1\cdot H_2^{2+}$. These are suggested as ICT bands from the 1,3-dithiole ring (D) to the protonated diazafluorene moiety (A), because solvatochromic shifts have been observed in the spectra of compound **4** ($L^1\cdot H^+$) in solvents with varying polarity (Figure 6a). The ICT-band peak shows solvatochromic shift from about 437 nm in acetonitrile to 462 nm in chloroform. However, solvatochromic shifts of the absorption peak have not been observed for compound L^1 (Figure 6b). The result reveals that the protonation enhances the charge separation and then increases the ICT effect.

Theoretical Calculations of the Electronic States for L^1, $L^1\cdot H^+$, and $L^1\cdot H_2^{2+}$. The study of electronic spectra provides some insight into the change of electronic states and indicates clearly the presence of D−A intramolecular CT for protonated L. To understand the nature of these CT bands, quantum chemical calculations were performed for the parent compound L^1 and the protonated cation $L^1\cdot H^+$ of **4** as well as $L^1\cdot H_2^{2+}$. All geometries were optimized by performing DFT calculations at the B3LYP/6-31G** level. The optimized structures of L^1 and $L^1\cdot H^+$ (Figure 3 in the SI) are similar to those found in the crystals. Comparing the experimental data with the calculated results for the main bond lengths and bond angles, only small differences were found between the crystal state and the gas-phase state for their rigid structure. Therefore, on the basis of the geometries of the compounds obtained from the full optimization computations, the studies on the molecular orbitals and related properties were further carried out with the DFT method.

Figure 7 displays the atomic orbital composition calculated for the highest occupied molecular orbitals (HOMO-1and HOMO) and the lowest unoccupied molecular orbital (LUMO) of L^1, $L^1\cdot H^+$, and $L^1\cdot H_2^{2+}$, respectively. For monoprotonated compound $L^1\cdot H^+$, the HOMO-1 is located over the dithiole moiety. The HOMO spreads over the whole molecule and results from the bonding of the diazafluorene moiety with the 1,3-dithiol-2-ylidene unit, while the LUMO is mostly located on the diazafluorene moiety. Hence the photoinduced HOMO−1-LUMO and HOMO−LUMO excitation should have a charge-transfer nature from the 1,3-dithiole moiety (D) to the protonated diazafluorene moiety (A), especially the change in electron density distribution from HOMO-1 to LUMO is large. The situation for diprotonated $L^1\cdot H_2^{2+}$ is similar to those found for monoprotonated $L^1\cdot H^+$. While for the unprotonated compound L^1, the orbital population of the 1,3-dithiole moiety of LUMO has only a slight change in comparison with that of HOMO. Therefore relative to L^1, $L^1\cdot H^+$ and $L^1\cdot H_2^{2+}$ are good ICT species.

A highly energetic HOMO−LUMO gap is indicative of the absence of a low-energy band in the visible region of the spectrum for compound L^1. The energy levels of the entire set of MOs of $L^1\cdot H^+$ dropped greatly due to the protonation, especially the LUMO, and a simultaneous reduction in energy gap ΔE ($E_{LUMO} - E_{HOMO}$) occurred. Thus, the lower energy gap results in the red shift of the absorption peak. For diprotonated $L^1\cdot H_2^{2+}$ the energy gap ΔE ($E_{LUMO} - E_{HOMO}$) is further degenerate and this correlates with the fact that the absorption spectra are red-shifted when compared to those of the monoprotonated $L^1\cdot H^+$.

According to the related orbital characters of $L^1\cdot H^+$, the HOMO-1→LUMO excitation was calculated at 2.82 eV (f = 0.34). The HOMO→LUMO excitation gives rise to the lowest energy gap 2.32 eV (f = 0.008). The electronic transition of HOMO→LUMO has very low intensity and causes an invisible absorption band, therefore the first visible band should be the HOMO-1→LUMO excitation (the ICT shoulder peak in Figure 5a, blue line). Similarly, for diprotonated species $L^1\cdot H_2^{2+}$ the first absorption band at about 580 nm is the most strong ICT band corresponding to the HOMO-1→LUMO excitation (Figure 7 bottom).

^{1}H NMR. The response of parent compound L^2 (**2**) to acid was measured by adding increasing amounts of CF_3SO_3H to a 0.2 M solution of **2** in $CDCl_3$. The ^{1}H NMR spectrum reveals

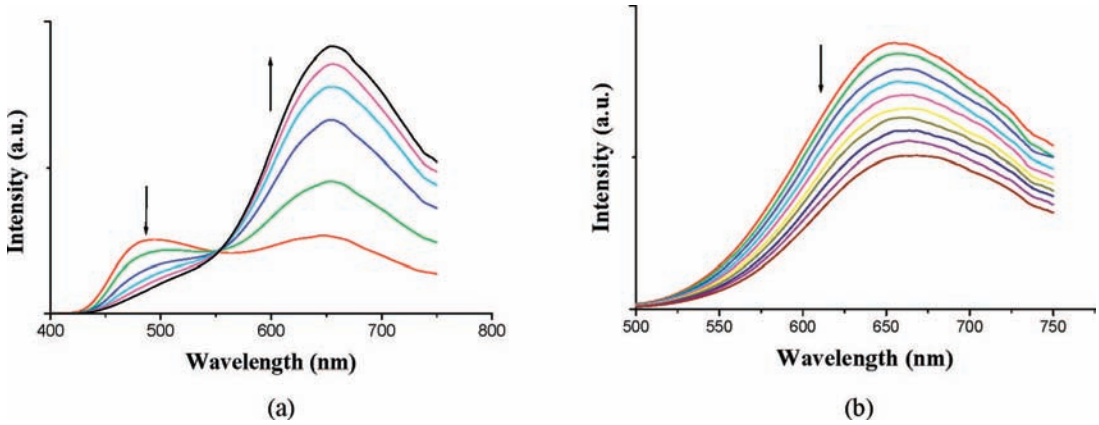

Figure 9. Fluorescence spectra of compound L^1 in CH_2Cl_2 upon addition of increasing amounts of CF_3SO_3H excited at 400 nm.

TABLE 1: Crystallographic and Refinement Data for Compounds 2−5

	2	3	4	5
formula	$C_{18}H_{16}N_2S_4$	$C_{19}H_{17}F_3N_2O_3S_5$	$C_{17}H_{13}F_3N_2O_3S_5$	$C_{33}H_{30}Cl_2N_4O_9S_8$
formula wt	388.57	538.65	510.59	953.99
crystal size (mm^3)	0.45 × 0.30 × 0.08	0.54 × 0.30 × 0.20	0.60 × 0.29 × 0.20	0.62 × 0.30 × 0.26
crystal system	triclinic	triclinic	monoclinic	triclinic
space group	$P\bar{1}$	$P\bar{1}$	$C2/c$	$P\bar{1}$
a (Å)	9.894(3)	9.1270(15)	21.068(5)	12.3485(8)
b (Å)	13.952(4)	11.4047(15)	14.014(3)	13.1326(10)
c (Å)	14.722(4)	11.9020(18)	14.368(3)	15.2098(13)
α (deg)	106.546(3)	71.207(11)	90.00	69.981(13)
β (deg)	106.556(3)	82.276(12)	106.740(3)	67.801(13)
γ (deg)	103.482(3)	79.411(12)	90.00	62.584(12)
V ($Å^3$)	1754.7(8)	1149.1(3)	4062.1(16)	1984.2(3)
Z	4	2	8	2
D_{calc} (mg m^{-3})	1.471	1.557	1.670	1.597
$F(000)$	808	552	2080	980
no. of refs collected	17328	11161	19191	17471
no. of unique data	6381	4159	3716	7026
goodness-of-fit (S)	1.147	1.077	1.115	1.116
R_1	0.0619	0.0495	0.0823	0.0599
wR_2	0.1125	0.1202	0.1856	0.1352

clearly three sets of hydrogen signals of the diazafluorene moiety located at 8.68, 8.07, and 7.39 ppm (Figure 8 bottom), respectively, which has been discussed in detail in our previous work.[6d] The proton signals of the diazafluorene moiety display a distinct downfield shift upon addition of acid, which can be attributed to the strong electron-withdraw property or the deshielding effect of the added proton. Whatever the amount of acid added is, shortfall or excess, the ^1H NMR spectrum always shows three set distinct signals of the diazafluorene moiety, which suggests fast shuttling of the proton between both nitrogen atoms of the diazafluorene moiety and between unprotonated L^2 and $L^2 \cdot H^+$ on the NMR time scale.[9b] The protonated structure of L^2 in solution is not in accord with the solid state structure in which the proton is fixed onto one of the two nitrogen atoms.

Fluorescence Spectra. Figure 9 shows the fluorescence spectra of compound L^1 in CH_2Cl_2 upon addition of increasing amounts of CF_3SO_3H. The emission signals of the parent compound L^1 appear at 486 nm (red line) (λ_{ex} = 400 nm). Addition of increasing amounts of CF_3SO_3H to a solution of L^1 in CH_2Cl_2 leads to the decrease of the band at 486 nm and a new emission band appears at 648 nm. The weak spectral fingerprint of 648 nm for the starting spectrum of L^1 might be due to some acid impurities in the CH_2Cl_2 solvent. Upon addition of acid to form $L^1 \cdot H^+$ completely, the intensity of the emission at 648 nm reaches the highest and the emission band at 486 nm disappears (Figure 9a). After this stage the emission intensity gradually quenches upon further addition of acid (Figure 9b). The turning point of the emission intensity corresponds to the transition from monoprotonated to diprotonated species, which is consistent with that of the UV−vis measurement.

Conclusions

In summary, we have studied the structure and spectral properties of a molecular system of diazafluorene derivatives with a sulfur-rich moiety of 4,5-dialkylthio-1,3-dithiol-2-ylidene. The substituents play an important part in modification of the electronic state (ICT) of the parent compound. As analogues of phenanthroline or bipyridine, these compounds can undergo two-step protonation in solution, whereas in solid state monoprotonated compounds they are isolated as stable crystals. Structural analysis showed that the protonated imine group forms strong N−H···O or N−H···N hydrogen bonds, which enhance the interaction between cations and anions and play an important role in the molecular packing. Spectral analysis reveals that electronic states and the absorption bands of these compounds are affected by protonation. Especially, the ICT property is significantly enhanced when the proton is added. Compound L is also a proton-sensible fluorescent system with two-step changes in band energy and intensity. Theoretical calculation with the DFT/TDDFT method has further complemented the study on the effect of protonation for this D−A system.

Experimental Section

General Remarks. All of the reagents for synthesis were commercially available and used as received without purification. The parent compounds L^1 (**1**) and L^2 (**2**) were synthesized by using a modified method reported by Sako.[12] The solvents for UV−vis and fluorescence spectra are HPLC grade from Alfa Aesar. Elemental analyses of C, H, and N were performed with an EA 1110 elemental analyzer. IR spectra were recorded on a Nicolet Magna 550 FT-IR spectrometer as KBr pellets. UV−vis spectra were recorded on a Shimadzu UV-3150 spectrometer. Fluorescence spectra were recorded on an Edinburgh FLS920 spectrometer. DFT calculations were carried out with the GAUSSIAN 03 program package.[13] All calculations were performed with B3LYP, together with the 6-31G** basis set.

Preparation and Crystal Growth. ***Crystals of L^2 (2).*** A powder sample of L^2 (7.8 mg, 0.02 mmol) was dissolved in dichloromethane (2 mL) and the solution was transferred into a glass tube. Methanol (2 mL) was added slowly to the tube along its inside wall. Yellow block-shaped crystals were obtained after a few weeks (4.7 mg, 60%). Important IR data: 1555 (m), 1540 (vs), 1480 (vs), 1393 (vs), 1173 (s), 856 (m), 802 (m) cm^{-1}. Anal. Calcd for $C_{18}H_{16}N_2S_4$: C, 55.67; H, 4.12; N, 7.22. Found: C, 55.46; H, 4.06; N, 7.18.

$[L^2 \cdot H]CF_3SO_3$ (3). A methanol solution (0.5 mL) of CF_3SO_3H (0.04 mmol, 3.6 μL) was added to a dichloromethane solution (1 mL) of L^2 (0.02 mmol, 7.7 mg). The mixture was stirred for 1.5 h at room temperature and then was injected into the bottom of a glass tube. Large red crystalline blocks of **3** suitable for X-ray diffraction were obtained by a diffusion method with ethyl ether (5.7 mg, 53%). Important IR data: 3075 (m), 1570 (m), 1520 (vs), 1472 (vs), 1401 (s), 1258 (s), 1153 (s), 859 (m), 808 (m) cm^{-1}. Anal. Calcd for $C_{19}H_{17}F_3N_2O_3S_5$: C, 42.38; H, 3.16; N, 5.20. Found: C, 42.23; H, 3.06; N, 5.17.

$[L^1 \cdot H]CF_3SO_3$ (4). Red block crystals of **4** were obtained by a similar procedure as for crystal **3** except that the solution of L^2 was replaced by a solution of L^1 (5.9 mg, 58%). Important IR data: 3091 (m), 1561 (m), 1530 (vs), 1475 (vs), 1401 (s), 1260 (s), 1168 (s), 859 (m), 807 (m) cm^{-1}. Anal. Calcd for $C_{17}H_{13}F_3N_2O_3S_5$: C, 40.00; H, 2.55; N, 5.49. Found: C, 39.89; H, 2.50; N, 5.38.

$[L^1 \cdot H]ClO_4 \cdot 0.5CH_3OH$ (5). Red block crystals of **5** were obtained by a similar procedure as for crystal **4** except that the solution of CF_3SO_3H was replaced by a solution of $HClO_4$ in a mixed solvent of methanol and water (5.3 mg, 56%). Important IR data: 3096 (m), 1564 (m), 1524 (s), 1464 (s), 1399 (s), 1088 (vs), 860 (m), 802 (m) cm^{-1}. Anal. Calcd for $C_{33}H_{30}Cl_2N_4O_9S_8$: C, 41.55; H, 3.17; N, 5.87. Found: C, 41.45; H, 3.11; N, 5.77.

X-ray Crystallographic Study. All measurements were carried out on a Rigaku Mercury CCD diffractometer at 293 K with graphite monochromated Mo Kα (λ = 0.71073 Å) radiation. X-ray crystallographic data for the compounds were collected and processed by using CrystalClear (Rigaku).[14] The structures were solved by direct methods with SHELXS-97[15a] and the refinements against all reflections of the compounds were performed with SHELXL-97.[15b] All the non-hydrogen atoms were refined anisotropically. The hydrogen atoms were positioned with idealized geometry and refined with fixed isotropic displacement parameters, except for the H^+ atom combined with one of the imine nitrogens in compound **3** and **4** that was observed by Fourier map. The relevant crystallographic data, collection parameters, and details of refinement results for compounds L^2 (**2**), $[L^2 \cdot H]CF_3SO_3$ (**3**), $[L^1 \cdot H]CF_3SO_3$ (**4**), and $[L^1 \cdot H] \cdot ClO_4$ (**5**) can be found in Table 1.

Acknowledgment. This work was supported by the National NSF (20371033), the NSF of the Education Committee of Jiangsu Province (Grant 06KJB150102), and the Doctoral Foundation of Soochow University.

Supporting Information Available: Crystallographic data for **2**−**5** in CIF format, figures of molecular packing, other UV−vis spectra, and CV results. This material is available free of charge via the Internet at http://pubs.acs.org.

References and Notes

(1) (a) Armaroli, N. *Chem. Soc. Rev.* **2001**, *30*, 113–124. (b) Marin, V.; Holder, E.; Hoogenboom, R.; Schubert, U. S. *Chem. Soc. Rev.* **2007**, *36*, 618–635. (c) Chelucci, G.; Thummel, R. P. *Chem. Rev.* **2002**, *102*, 3129–3170. (d) Kaes, C.; Katz, A.; Hosseini, M. W. *Chem. Rev.* **2000**, *100*, 3553–3590. (e) Vlček, A.; Busby, M. *Coord. Chem. Rev.* **2006**, *250*, 1755–1762.

(2) (a) Medlycott, E. A.; Hanan, G. S. *Chem. Soc. Rev.* **2005**, *34*, 133–142. (b) Silva, A. P.; Fox, D. B.; Huxley, A. J. M.; Moody, T. S. *Coord. Chem. Rev.* **2000**, *205*, 41–57. (c) Beer, P. D.; Cadman, J. *Coord. Chem. Rev.* **2000**, *205*, 131–155. (d) Bossert, J.; Daniel, C. *Coord. Chem. Rev.* In press. (e) Juris, A.; Balzani, V.; Barigelletti, F.; Campagna, S.; Balser, P.; Zelewsky, V. *Coord. Chem. Rev.* **1988**, *84*, 85–277.

(3) (a) Belser, P.; Cola, L. D.; Hartl, F.; Adamo, V.; Bozic, B.; Chriqui, Y.; Lyer, V. M.; Jukes, R. T. F.; Kühni, J.; Querol, M.; Roma, S.; Salluce, N. *Adv. Funct. Mate.* **2006**, *16*, 195–208. (b) Wong, K.-T.; Chen, H.-F.; Fang, F.-C. *Org. Lett.* **2006**, *8*, 3501–3504. (c) Su, H.-C.; Chen, H.-F.; Wu, C.-C.; Wong, K.-T. *Chem. Asian J.*, DOI: 10.1002/asia.200800020.

(4) (a) Sans, M. Q.; Belser, P. *Coord. Chem. Rev.* **2002**, *229*, 59–66. (b) Wong, W.-Y. *Coord. Chem. Rev.* **2005**, *249*, 971–997.

(5) (a) Warrener, R. N.; Ferreira, A. B. B.; Schultz, A. C.; Butler, D. N.; Keene, F. R.; Kelso, L. S. *Angew. Chem., Int. Ed.* **1996**, *35*, 2485–2487. (b) Kraft, B. J.; Eppley, H. J.; Huffman, J. C.; Zaleski, J. M. *J. Am. Chem. Soc.* **2002**, *124*, 272–280.

(6) (a) Zhu, Q.-Y.; Dai, J.; Jia, D.-X.; Cao, L.-H.; Lin, H.-H. *Eur. J. Inorg. Chem.* **2004**, 4789–4794. (b) Zhu, Q.-Y.; Lu, W.; Zhang, Y.; Bian, G.-Q.; Gu, J.; Lin, X,-M.; Dai, J. *Eur. J. Inorg. Chem.* **2008**, 230–238 (c) Zhu, Q.-Y.; Bian, G.-Q.; Dai, J.; Jia, D.-X.; Zhang, J.-S. *Inorg. Chem. Acta* **2003**, *351*, 177–182. (d) Zhu, Q.-Y.; Dai, J.; Jia, D.-X.; Cao, L.-H.; Lin, H.-H. *Polyhedron* **2004**, *23*, 2259–2264. (e) Zhu, Q.-Y.; Zhang, Y.; Dai, J.; Bian, G.-Q.; Jia, D.-X. *Chem. Lett.* **2003**, *8*, 762–763.

(7) Grabowski, Z. R.; Rotkiewicz, K.; Rettig, W. *Chem. Rev.* **2003**, *103*, 3899–4032.

(8) Pan, J.-F.; Chen, Z.-K.; Chua, S.-J.; Huang, W. *J. Phys. Chem. A* **2001**, *105*, 8775–8781.

(9) (a) Armaroli, N.; De Cola, L.; Balzani, V.; Sauvage, J. P.; Dietrich-Buchecker, C. O.; Kern, J. M. *J. Chem. Soc., Faraday Trans.* **1992**, *88*, 553–556. (b) Dietrich-Buchecker, C. O.; Sauvage, J. P.; Armaroli, N.; Ceroni, P.; Balzani, V. *New J. Chem.* **1996**, *20*, 801. (c) Armaroli, N.; Ceroni, P.; Balzani, V.; Kern, J. M.; Sauvage, J. P.; Weidmann, J. L. *J. Chem. Soc., Faraday Trans.* **1997**, *93*, 4145–4150. (d) Armaroli, N. *Photochem. Photobiol. Sci.* **2003**, *2*, 73–87. (e) Listorti, A.; Degli Esposti, A.; Kishore, R. S. K.; Kalsani, V.; Schmittel, M.; Armaroli, N. *J. Phys. Chem. A* **2007**, *111*, 7707–7718.

(10) Zhu, Q. Y.; Liu, Y.; Lu, W.; Zhang, Y.; Bian, G. Q.; Niu, G. Y.; Dai, J. *Inorg. Chem.* **2007**, *46*, 10065–10070.

(11) Kulkarni, P.; Padhye, S.; Sinn, E. *Inorg. Chim. Acta* **2001**, *321*, 193–199.

(12) Sako, K.; Kusakabe, M.; Tatemitsu, H. *Mol. Cryst. Liq. Cryst.* **1996**, *285*, 101–106.

(13) (a) *Gaussian 03*, revision C.01; Gaussian, Inc.: Wallingford, CT, 2004. (b) Becke, A. D. *J. Chem. Phys.* **1993**, *98*, 5648–5652.

(14) Rigaku Corporation, 1999; *CrystalClear Software User's Guide*; Molecular Structure Corporation, 2000. Pflugrath, J. W., *Acta Crystallogr., Sect. D*, **1999**, *55*, 1718−1725.

(15) (a) Sheldrick, G. M. *SHELXS-97*, Program for structure solution; Universität of Göttingen: Göttingen, Germany, 1999. (b) Sheldrick, G. M., *SHELXL-97*, Program for structure refinement; Universität of Göttingen: Göttingen, Germany, 1997.

JP8073283